Supporting Information

Yang *et al.* 10.1073/pnas.0711845105

SI Materials and Methods

Live Imaging of Mitochondrial Morphology in COS-7 Cells and S2R Cells. COS-7 cells were cultured in DMEM supplemented with 10% FCS and nonessential amino acids (Invitrogen) and plated on cover glass in a 37°C incubator. All constructs described here contain the CMV promoter and the specified epitope tags. hPink1-Flag, hPink1ΔC-Flag, Myc-hFis1, and Drp1-Myc constructs (1.0 μg of DNA for each construct in 200 μl of culture medium) were introduced into COS-7 cells with Fugene 6 (Roche) according to manufacturer-recommended protocols. For *hPink1* RNAi in COS-7 cells, two shRNA constructs (TRCN0000007099 and DsTRCN0000007101) (Open Biosystems) targeting hPink1-coding sequences (1.5 μg of DNA for each construct in 200 μl of culture medium) were introduced into cells with Fugene 6 (Roche). Sixty hours after transfection, the cells with incubated with 25 nM Mitotracker CMX-Ros Red (MTRed dye) (Invitrogen) at 37°C for 1 h and then rinsed with complete culture medium twice. Observation was started 15 min after the completion of MTRed dye staining for monitoring the effect of the genetic manipulations on mitochondrial fusion, with cells exhibiting type II and III (fusion) or V and VI (fission) mitochondrial morphology scored. To facilitate the scoring of effects of genetic manipulations on mitochondrial fission, observation was started 2–3 h after the completion of MTRed dye staining, with cells exhibiting type II and III (fusion) and V and VI (fission) mitochondrial morphologies scored. The 2- to 3-h incubation after MTRed dye staining resulted in more cells with tubular (or fused) mitochondria (Fig. S7), facilitating the scoring of fission events. This change in mitochondrial morphology due to culture condition is physiological, because it is reproducible and reversible. Because of the mixed fission and fusion characteristics of type IV and the low frequency of type I and VII, they were not included in the statistical analysis.

At the time of scoring, we first examined the transfected cells in one particular order in the first round. We then examined them randomly in the second round. Each scoring took ≈1–1.5 min. The whole process was completed in 25–30 min. Within this time frame, the mitochondrial morphology does not show significant changes. For each condition, at least four independent experiments had been performed, and in each experiment, we prepared duplicates of transfected cells.

S2R cells [a gift from Jun Zhang and Matthew Scott (Department of Developmental Biology, Stanford University, Stanford, CA)] were cultured in Schneider's medium supplemented with 10% heat-inactivated FBS (Sigma-Aldrich) and plated on cover glass in a 25°C incubator. EFGP and EGFP-dFis1 constructs (0.75 μg of DNA for each construct in 200 μl of culture medium) were introduced into S2R cells with Fugene 6 (Roche) according to manufacturer-recommended protocols. For RNAi experiments, 1 μg of dsRNA of individual targeted genes was applied onto S2R cells with Fugene 6 in a final volume of 150 μl of culture medium. Seventy-two hours after transfection, cells were incubated with 25 nM MT Red at 25°C for 1 h, and then rinsed with complete culture medium twice. Observation was initiated immediately after rinse.

Visualizing Mitochondria in Fly DA Neurons. Whole-mount immunohistochemistry for TH and GFP staining was performed as described in ref. 1. An antibody against TH (2) and a commercial antibody against GFP (Invitrogen) were used. An average of eight flies for each genotype per time point was examined, and each experiment was repeated at least three times.

For quasi-live imaging of mitochondria in DA neurons, adult brains were dissected out of head cuticles in 4% formaldehyde in PBS at room temperature, fixed briefly for 6 min, and then mounted for fluorescence microscopic observation. Because mitochondrial morphology is sensitive to overall environmental conditions, variations did occur from batch to batch. We only compared flies of different genotypes if normal mitochondrial morphology (refer to Fig. 2*A*) was observed in the control samples processed under the same conditions in the same batch. Experiments with proper controls were repeated more than five times. For data quantification of mitochondrial aggregation, in each experiment, ≈150 DA neurons of 10 PPL clusters were scored for each genotype. To facilitate phenotypic scoring, mitochondrial aggregates were separated into two groups based on their size, those between 1 and 2 μm and those >2 μm in diameter. The percentage of DA neurons containing mitochondrial aggregates belonging to the two categories was quantified.

The neuronal culture system was established and processed as described in ref. 3. Mito-GFP was driven by the TH promoter, which allowed us to visualize mitochondria directly in cultured DA neurons. Only neurons grown under similar culture conditions, in terms of cellular density and surrounding environment, were chosen to investigate DA neuron mitochondrial morphology among experiments. Only those TH^+ neurons with more than one tubular mitochondrial threads (shown in Fig. 3*J*) were used for statistical analysis shown in Fig. 3*K*. Tubular neuritic mitochondria were defined as those mitochondria units longer than 10 pixels. Each experiment was performed at least three times.

1. Pesah Y, Pham T, Burgess H, Middlebrooks B, Verstreken P, Zhou Y, Harding M, Bellen H, Mardon G (2004) *Drosophila* parkin mutants have decreased mass and cell size and increased sensitivity to oxygen radical stress. *Development* 131:2183–2194.
2. Yang Y, Gehrke S, Imai Y, Huang Z, Ouyang Y, Wang JW, Yang L, Beal MF, Vogel H, Lu B (2006) Mitochondrial pathology and muscle and dopaminergic neuron degeneration caused by inactivation of *Drosophila* Pink1 is rescued by Parkin. *Proc Natl Acad Sci USA* 103:10793–10798.
3. Yang Y, Nishimura I, Imai Y, Takahashi R, Lu B (2003) Parkin suppresses dopaminergic neuron-selective neurotoxicity induced by Pael-R in *Drosophila*. *Neuron* 37:911–924.

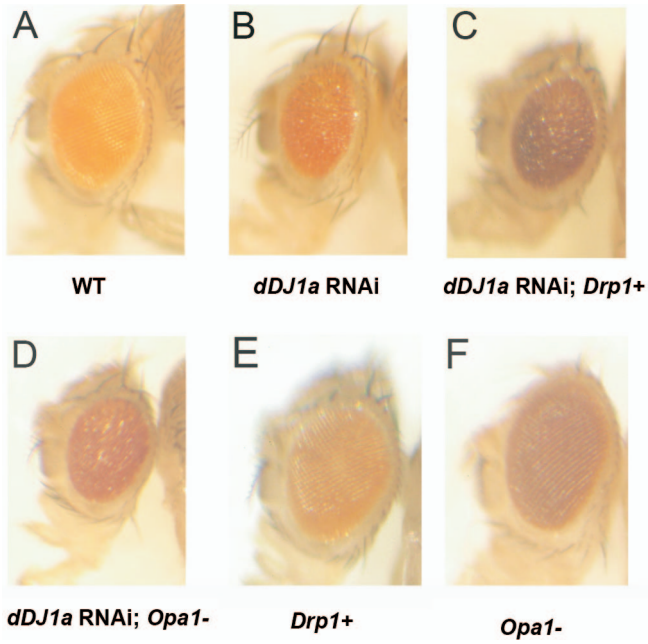

Fig. S1. No rescue of DJ-1a RNAi-induced retinal degeneration after up-regulation of mitochondrial fission. Light-microscopic images of 5-day-old adult fly eyes of the following genotypes are shown: *GMR-Gal4/+* (*A*), *GMR-Gal4>DJ-1a RNAi* (*B*), *GMR-Gal4>DJ-1a RNAi; Drp1 extra* (*C*) and *GMR-Gal4>DJ-1a RNAi; Opa1-like/+* (*D*), *Drp1 extra* (*E*), and *Opa1-like/+* (*F*). Inhibition of DJ-1a by RNAi resulted in rougher and smaller-sized eye (*B*), which was not modified in *C* or *D*. Note that *Drp1 extra* (*E*) and *Opa1-like/+* (*F*) flies have normal eye morphology. The spotted appearance in *E* and *F* is due to light reflection.

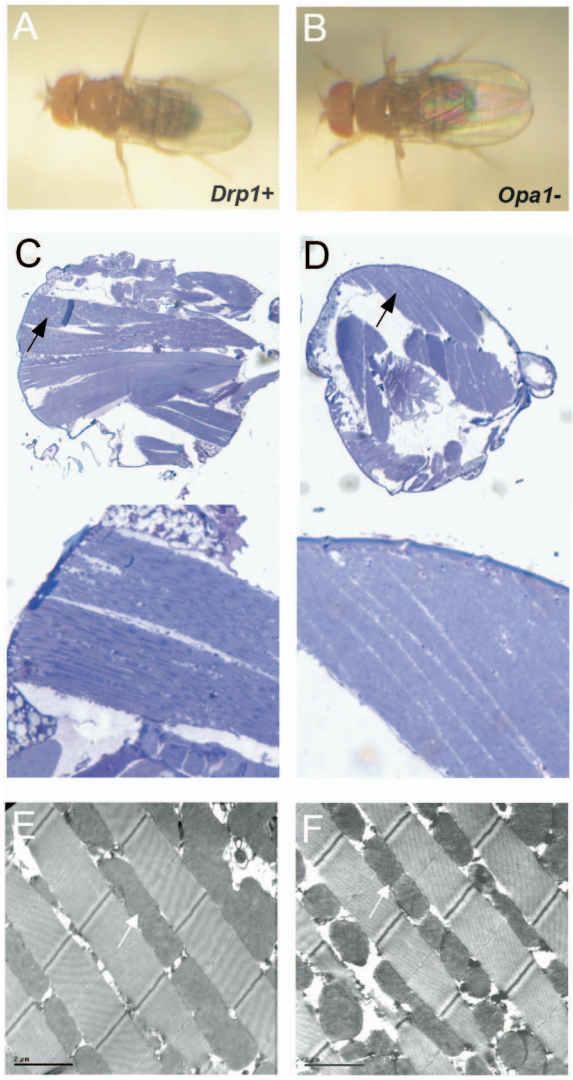

Fig. S2. Lack of effect on IFM muscle organization and mitochondrial morphology in animals carrying an extra copy of Drp1 or heterozygous for Opa1-like in an otherwise wild-type background. (*A* and *B*) Normal wing posture in adult flies of *Drp1 extra copy* (*A*) and *Opa1-like*/+ (*B*). (*C* and *D*) Longitudinal sections of thoraces in 5-day-old *Drp1 extra copy* (*C*) and *Opa1-like*/+ (*D*) flies. The lower images display magnified views of IFMs. Sections from resin-embedded thoraces were stained with toluidine blue to visualize tissue morphology, particularly the musculatures; anterior is to the left. (*E* and *F*) Transmission electronic microscopy analysis of IFM ultrastructure in 5-day-old *Drp1 extra copy* (*E*) and *Opa1-like*/+ (*F*) flies.

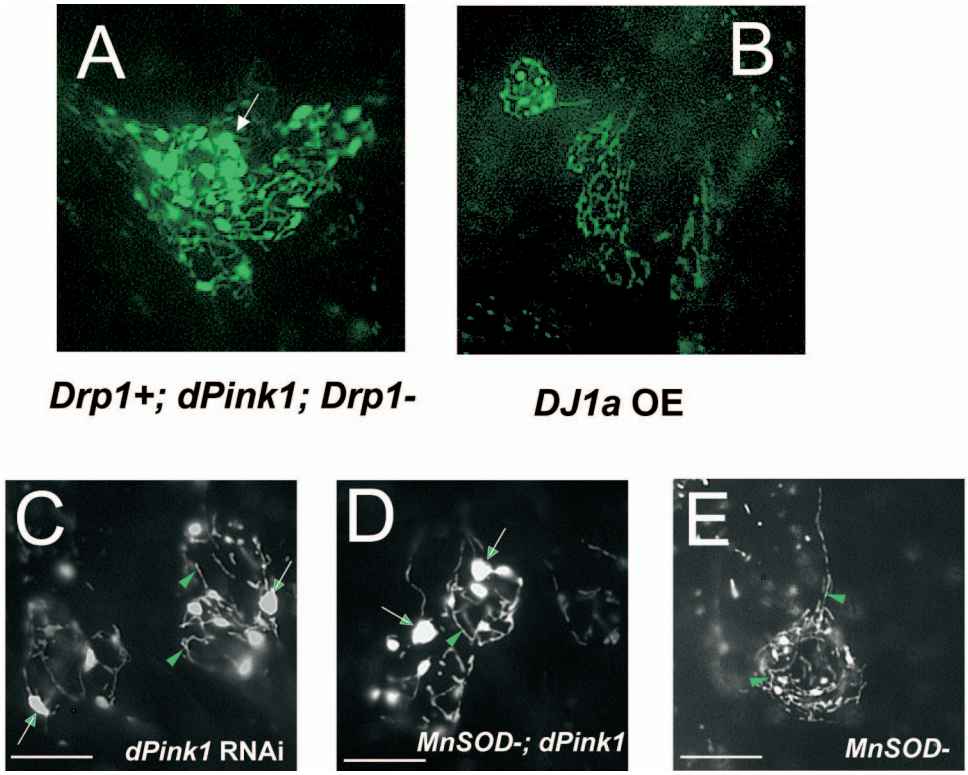

Fig. S3. Quasi-live imaging of mitochondrial morphology in *dPink1* mutant flies with Drp1 gene dosage restored to normal or in DJ-1a overexpression animals. (*A*) In 5- to 7-day-old adult flies of *TH-Gal4>UAS-mitoGFP; B9; Drp1 extra; Drp1/+* animals, abnormal mitochondrial aggregation in PPL1 cluster dopaminergic neurons is still present, whereas in *TH-Gal4>UAS-mitoGFP; B9; Drp1 extra* animals the mitochondrial abnormality is suppressed (see Fig. 2*F*), indicating that Drp1 gene dosage is important for the rescuing effect. (*B*) Mitochondrial morphology in PPL1 cluster dopaminergic neurons of *TH-Gal4>UAS-mitoGFP; UAS-DJ-1a* animals appears normal. (*C–E*) The mitochondrial aggregation phenotype in *TH-Gal4>UAS-mitoGFP; B9* (*C*) was not modified by the removal of one copy of the mitochondrial *MnSODII* gene (*D*). Loss of one copy of the mitochondrial *MnSODII* gene in a wild-type background also had no effect on mitochondrial morphology (*E*). The arrows mark mitochondrial aggregates, and the arrowheads mark tubular mitochondria.

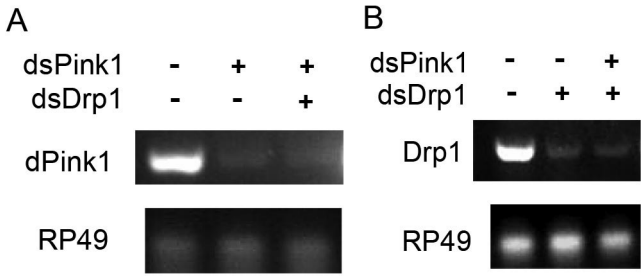

Fig. S4. RT-PCR analysis of RNAi effect in S2R cells. (*A*) Cells subjected to control RNAi, *dPink1* RNAi, or *dPink1* + *Drp1* RNAi were analyzed for *dPink1* mRNA level by RT-PCR. (*B*) Cells subjected to control RNAi, *Drp1* RNAi, or *dPink1* + *Drp1* RNAi were analyzed for *Drp1* mRNA level by RT-PCR. *RP49* serves as an internal control for input total mRNA.

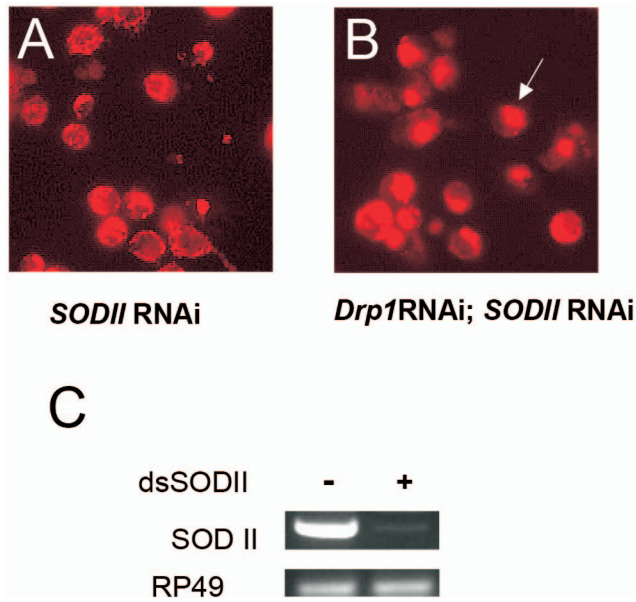

Fig. S5. Lack of modifying effect by *MnSODII* RNAi on *Drp1* RNAi-induced mitochondrial abnormality in S2 cells. (*A* and *B*) MitoTracker live imaging of mitochondria in S2R cells subjected to *MnSODII* RNAi (*A*) or *Drp1* RNAi plus *MnSOD II* RNAi (*B*). (*C*) RT-PCR analysis showing the efficiency of RNAi knockdown of *MnSODII* RNA level. This result serves as a control to show that the unique appearance of continuous mitochondrial tubules observed in cells subjected to double knockdown of *Pink1* and *Drp1* results from specific interaction between Pink1 and Drp1 in regulating mitochondrial fission, rather than a nonspecific effect of attenuation of normal mitochondrial function.

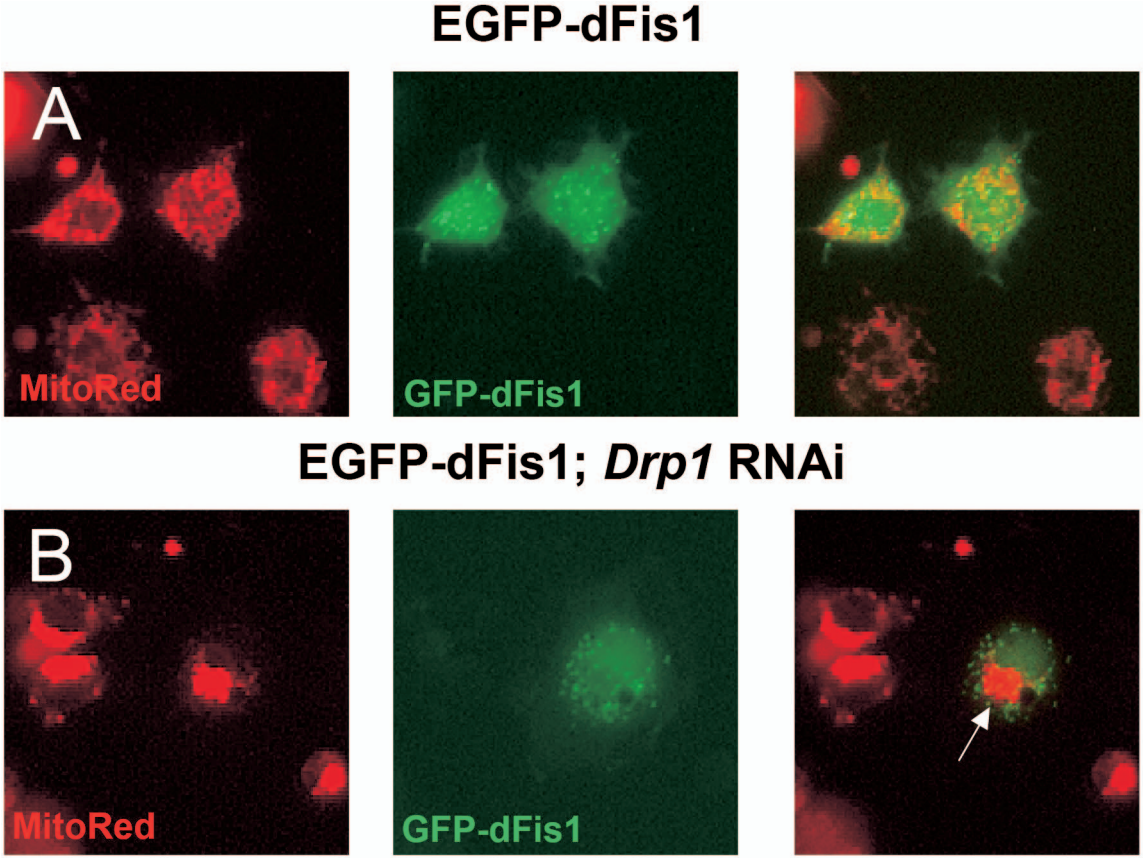

Fig. S6. EGFP-dFis1 overexpression fails to suppress *Drp1* RNAi-induced mitochondrial aggregation in S2R cells. (*A*) Cells transfected with N-terminal EFGP-dFis1 fusion protein exhibit normal mitochondrial morphology. (*B*) The presence of EGFP-dFis1 does not modify the mitochondrial aggregation phenotype caused by Drp1 RNAi. The left images display MitoTracker Red staining, and the center images show transfected $EGFP^{+}$ cells. Merged images are shown on the right.

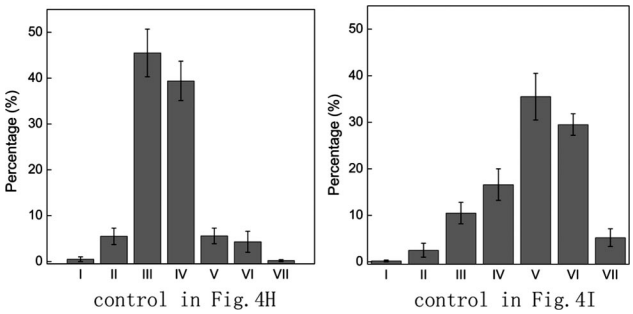

Fig. S7. Statistical analysis showing the relative distribution of the seven categories of mitochondrial phenotypes in the control cells used in Fig. 4 *H* and *I*. Note that, when Cos-7 cells were analyzed 2–3 h after incubation with MitoTracker Red at room temperature, mitochondrial fusion rate was increased, as indicated by the increased frequency of category II and III phenotypes (left chart). This condition was used to facilitate the assessment of the effect of hPink1 overexpression on mitochondrial fission. Cos-7 cells show an intrinsically high fission rate when analyzed 15 min after MitoTracker Red staining, as indicated by the predominant category V and VI phenotypes (right chart). This condition was used to facilitate the assessment of the effect of hPink1 RNAi on mitochondrial fusion.

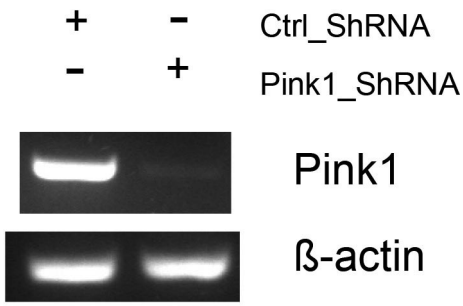

Fig. S8. RT-PCR analysis showing the efficiency of hPink1 RNAi in Cos-7 cells. Cos-7 cells transfected with control shRNA or hPink1 shRNA were used to prepare total RNA for RT-PCR analysis of hPink1 mRNA level. β-Actin was used as the internal control of mRNA input.

Table S1. Genetic manipulations of *Drp1* modulate the wing phenotype induced by *dPink1* RNAi

Genotypes	Penetrance of abnormal wing phenotype, %
Control	7.3 ± 2.5
MHC-Gal4; *dPink1* RNAi	55.6 ± 6.8
MHC-Gal4; *dPink1* RNAi, *Drp1* extra	8.1 ± 3.7
MHC-Gal4; *dPink1* RNAi, *Drp1* het. null	92.5 ± 4.6

Fourteen-day-old adult flies from each genotype kept at 29°C were scored. Phenotypic penetrance was then determined and presented in the format of average ± SD. *dPink1* RNAi was specifically induced in fly muscle by using the *myosin heavy chain (Mhc)-Gal4* driver. Drp1 extra, animals carrying an extra copy of Drp1 gene; Drp1 het. null, animals heterozygous for a *Drp1* null mutation.

Table S2. Age dependency of the rescuing effects of *Drp1* or *Opa1-like* genetic manipulations on *dPink1* null mutation

Genotypes	Phenotypic penetrance, %	
	10 days	1 month
dPink1 Null	80.5 ± 5.4	95.8 ± 3.2
dPink1 Null + *Drp1* extra	7.5 ± 2.6	15.3 ± 5.6
dPink1 Null + *Opa1* like het. null	10.3 ± 3.1	75.8 ± 5.2
Control	8.2 ± 2.7	10.1 ± 2.5

Ten-day- and 1-month-old adult flies from each genotype kept at 25°C were scored. Phenotypic penetrance was then determined and presented in the format of average ± SD. Opa1-like het. null, animals heterozygous for a *Opa1-like* null mutation.